

Supporting Information

Diphenylanthracene-based Trimeric Systems for Efficient Photon Upconversion through Triplet-Triplet Annihilation

Alisha Sengupta,^{†a} Sakura Nakagawa,^{†b,c} Aakash Ravikant Likhar,^a Masanori Uji,^{b,c} Nobuhiro Yanai^{*c} and Deepak Asthana^{*a}

^aDepartment of Chemistry, Ashoka University, Sonapat, Haryana, 131029, India; E-mail: deepak.asthana@ashoka.edu.in

^bDepartment of Chemistry, Graduate School of Science, The University of Tokyo, Japan; E-mail: yanai@chem.s.u-tokyo.ac.jp

^cDepartment of Chemistry, Graduate School of Science, The University of Tokyo, Japan.

Contents

.....

Sr. No.	Topic	Page No.
1	Experimental Section: General Information	S1-S4
	1.1 Materials and characterization methods	
	1.2 Fluorescence and triplet lifetime measurement method	
	1.3 TTA-UC measurement conditions and schematic diagram of setup and TTA-UC process	
	1.4 Fitting parameters for threshold value (I_{th}) calculations	
	1.5 Control experiments with DPA-PtOEP and 9-PA-PtOEP system	
2	Synthetic procedure for compounds 1 , 2 and 3	S4-S6
3	Concentration dependent UV-Vis. Absorption & emission spectra	S6
4	Concentration dependent ¹ H NMR spectra of 3	S7
5	Geometry optimized molecular structures of 1-3	S8
6	¹ H-NMR Spectra	S9-S10
7	¹³ C NMR Spectra	S11-S12
8	Mass Spectra	S12-S13
9	References	S14

1. General Information

1-1. Materials

All reagents from commercial sources were used without further purification unless otherwise stated. All chemicals were obtained from Sigma Aldrich and TCI chemicals. Thin layer chromatography (TLC) was carried out on aluminium plates coated with silica gel mixed with fluorescent indicator having particle size of 25 μm and was sourced from Merck India. Chloroform (CHCl_3) and triethylamine (NEt_3) were dried on calcium hydride. 9-bromoanthracene, 9-bromo-10-phenylanthracene, 4-carboxyphenylboronic acid, 4-aminophenylboronic acid pinacol ester, 1,3,5-benzenetricarbonyl trichloride, 1-ethyl-3-(3-dimethylaminopropyl)carbodiimide hydrochloride (EDC.HCl), hydroxybenzotriazole (HOBt), 1, 3, 5-benzenetricarboxylic acid and tris(2-aminoethyl)amine were purchased from TCI Chemicals. K_2CO_3 , ethanol and toluene were obtained from SRL Chemicals. Tetrakis(triphenylphosphine)palladium(0) and N, N-dimethylformamide (DMF) anhydrous, 99.8 % were obtained from Sigma Aldrich. NMR spectra were recorded at room temperature conditions using a 400 MHz Bruker spectrometer. MALDI-MS was done using Bruker Daltonics FLEX-PC (Autoflex-TOF) and α -cyano-4-hydroxycinnamic acid (CHCA) matrix. UV-Vis. Absorption spectra were recorded using an Agilent Cary-60 Spectrophotometer. PL spectra were recorded using HORIBA CANADA QM-8450-22-C. The absolute photoluminescence quantum yield was measured in an integrating sphere using a HAMAMATSU multichannel analyser C10027-01.

1-2. Fluorescence and triplet lifetime measurements

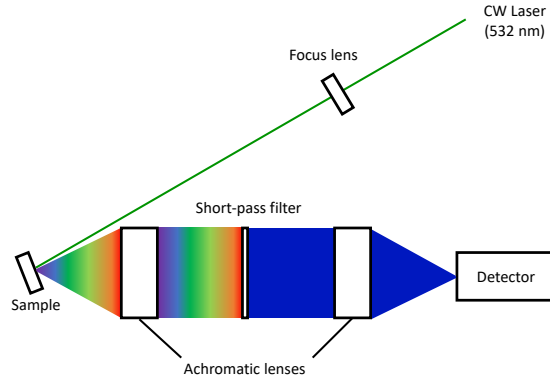
Time-resolved photoluminescence lifetime measurements were performed using a time-correlated single-photon counting lifetime spectroscopy system, HAMAMATSU QuantaTaurus-Tau C11367-21, C11567-02, and M12977-01. Internal TTA-UC efficiency (η_{UC}) was determined by the relative method. Excitation was performed using instrument's pulsed xenon lamp and the output intensity was automatically regulated by the software. The instrument response function (IRF) has a full-width at half-maximum (FWHM) of <100 ps (after deconvolution). All decay curves were analysed by deconvolution fitting with IRF to extract accurate triplet lifetimes.

1-3. TTA-UC measurements

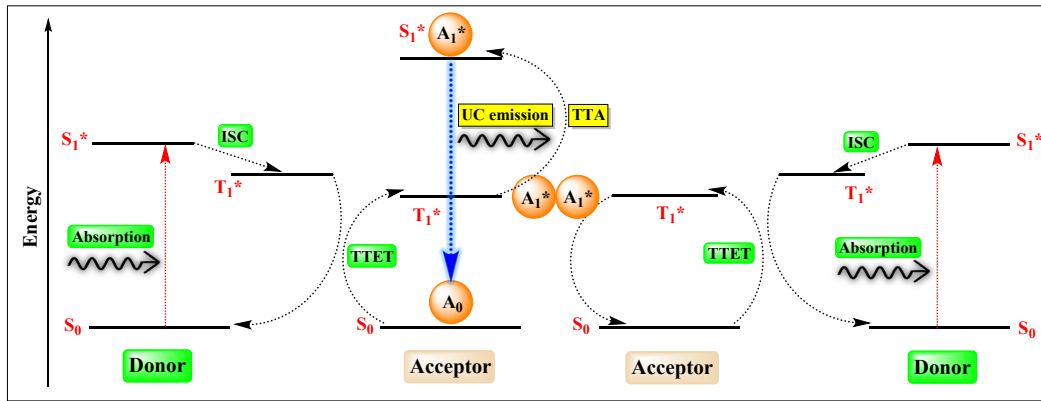
For TTA-UC measurements, samples were prepared in an argon (Ar) filled glove box ($[\text{O}_2] < 0.1 \text{ ppm}$) using a deoxidized THF solvent, purchased from FUJIFILM Wako. Solutions were transferred into 1 mm pathlength quartz cuvettes sealed with PTFE septa.

A 532 nm diode laser (75 mW, RGB Photonics) was used as the excitation light source. The laser power was controlled by combining a software (L-tune) and a variable neutral density filter, and power was measured using a PD300-UV photodiode sensor (OPHIR Photonics). The laser beam was focused on a sample using a lens. The diameters of the laser beam ($1/e^2$) were measured at the sample position using a CCD beam profiler SP620 (OPHIR Photonics). A typical area of the laser beam spot estimated from the diameter was $3.0 \times 10^{-4} \text{ cm}^2$ at the sample position. The laser power was controlled by rotating

variable ND filters, and the emission was focused by an achromatic lens to an optical fiber connected to a multichannel detector MCPD-9800 (Otsuka Electronics). A 510 nm short-pass filter was used between the sample and the detector. The detector was calibrated using a standard lamp Ocean Optics HL-3 plus-CAL.



Scheme S1. Schematic diagram of the TTA-UC measurement setup.



Scheme S2: Schematic representation of TTA-UC with relevant states and processes.

The TTA-UC efficiency (η_{UC}) in deaerated THF was determined relative to a Rhodamine 101 (25 μ M) in ethanol as a standard according to the following equation,^[4,5]

$$\eta_{UC} = 2\Phi_{std} \left(\frac{1 - 10^{-A_{std}}}{1 - 10^{-A_{UC}}} \right) \left(\frac{E_{UC}}{E_{std}} \right) \left(\frac{I_{std}}{I_{UC}} \right) \left(\frac{n_{UC}}{n_{std}} \right)^2$$

where Φ , A , E , I and n represent quantum yield, absorbance at 532 nm, excitation intensity, integrated photoluminescence spectral profile, and refractive index of the solvent, respectively. Note that the theoretical maximum of η_{UC} is normalized to be 1 (100%).

Fitting for TTA-UC lifetime was performed by following equations.^[6]

$$I_{UC}(t) \propto [T_{1,E}]^2 = \left([T_{1,E}]_0 \frac{1 - \beta}{\exp(t/\tau_T) - \beta} \right)^2 + B$$

where $I_{UC}(t)$ is the emission intensity, $[T_{1,E}]$ is the triplet concentration, t is the time, and β is the dimensionless parameter indicating the TTA efficiency ($0 < \beta < 1$).

1-4. Fitting parameters for threshold value (I_{th}) calculations

a) 1 $I_{th,1} = 2348.8 \text{ mW cm}^{-2}$ b) 2 $I_{th,2} = 118.2 \text{ mW cm}^{-2}$ c) 3 $I_{th,3} = 36.4 \text{ mW cm}^{-2}$

Equation	$y = a + b \cdot x$
Weight	No Weighting
Intercept	-10.9816 ± 0.17056
Slope	2.03119 ± 0.07148
Residual Sum of Squares	0.00406
Pearson's r	0.99753
R-Square (COD)	0.99507
Adj. R-Square	0.99384
Number of data plots	4

Equation	$y = a + b \cdot x$
Weight	No Weighting
Intercept	-7.8277 ± 0.11645
Slope	1.09555 ± 0.02617
Residual Sum of Squares	4.74303×10^{-4}
Pearson's r	0.99943
R-Square (COD)	0.99886
Adj. R-Square	0.99829
Number of data plots	6

Equation	$y = a + b \cdot x$
Weight	No Weighting
Intercept	-9.83079 ± 0.158
Slope	2.08002 ± 0.10496
Residual Sum of Squares	1.83761×10^{-4}
Pearson's r	0.99873
R-Square (COD)	0.99746
Adj. R-Square	0.99492
Number of data plots	5

Equation	$y = a + b \cdot x$
Weight	No Weighting
Intercept	-7.68211 ± 0.06195
Slope	1.01053 ± 0.01764
Residual Sum of Squares	4.91433×10^{-4}
Pearson's r	0.99939
R-Square (COD)	0.99878
Adj. R-Square	0.99848
Number of data plots	6

Equation	$y = a + b \cdot x$
Weight	No Weighting
Intercept	-8.51247 ± 0.13717
Slope	2.02598 ± 0.19185
Residual Sum of Squares	0.00808
Pearson's r	0.98682
R-Square (COD)	0.9738
Adj. R-Square	0.96507
Number of data plots	5

Equation	$y = a + b \cdot x$
Weight	No Weighting
Intercept	-6.91619 ± 0.05276
Slope	1.00371 ± 0.01515
Residual Sum of Squares	7.26989×10^{-5}
Pearson's r	0.99977
R-Square (COD)	0.99954
Adj. R-Square	0.99932
Number of data plots	4

Figure S1. Figures (a-c) showing the statistical parameters for the fitting of the excitation intensity ($\lambda_{ex} = 532 \text{ nm}$) vs. UPCL intensity plots obtained for upconversion samples (in deaerated THF) of molecules **1-3** [$100 \mu\text{M}$] and PtOEP [$1 \mu\text{M}$], respectively. Crossing point of fitted lines provides the threshold (I_{th}) values.

1-5. DPA-PtOEP and 9-PA-PtOEP system:

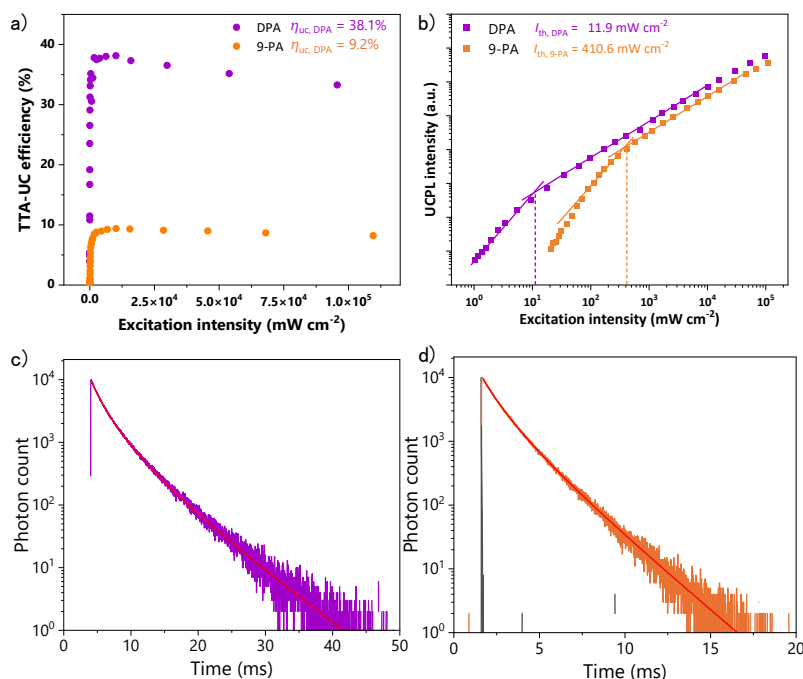


Figure S2: TTA-UC studies of DPA [$300 \mu\text{M}$]-PtOEP [$1 \mu\text{M}$] and 9-PA [$300 \mu\text{M}$]-[PtOEP $1 \mu\text{M}$] systems in deaerated THF ($\lambda_{ex} = 532 \text{ nm}$, 470 nm short-pass filter). (a) TTA-UC efficiency η_{UC} at different excitation intensities. (b) Excitation intensity dependence of double-logarithmic scale of upconversion photoluminescence at 425 nm and threshold values. (c) Triplet lifetime ($\tau_T = 10.8 \text{ ms}$) of DPA-PtOEP system. (d) Triplet lifetime ($\tau_T = 2.3 \text{ ms}$) of 9-PA-PtOEP system.

a) DPA $I_{th, DPA} = 11.9 \text{ mW cm}^{-2}$ b) 9-PA $I_{th, 9-PA} = 410.6 \text{ mW cm}^{-2}$

Equation	$y = a + b \cdot x$
Plot	UCPL intensity
Weight	No Weighting
Intercept	-6.15361 ± 0.02786
Slope	1.00006 ± 0.00731
Residual Sum of Squares	6.24844×10^{-5}
Pearson's r	0.99992
R-Square (COD)	0.99984
Adj. R-Square	0.99979

Equation	$y = a + b \cdot x$
Plot	UCPL intensity
Weight	No Weighting
Intercept	-7.27515 ± 0.04726
Slope	2.04392 ± 0.09959
Residual Sum of Squares	0.00526
Pearson's r	0.99646
R-Square (COD)	0.99293
Adj. R-Square	0.99057

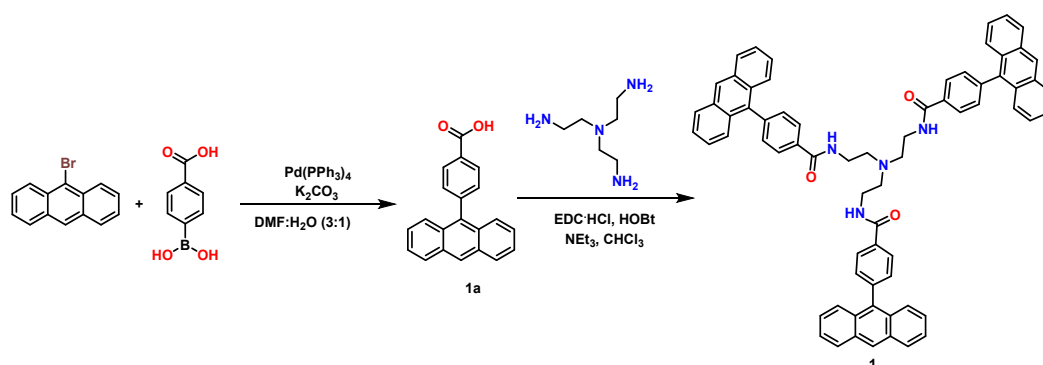
Equation	$y = a + b \cdot x$
Plot	UCPL intensity
Weight	No Weighting
Intercept	-6.42917 ± 0.05825
Slope	1.00233 ± 0.01443
Residual Sum of Squares	2.39296×10^{-4}
Pearson's r	0.99969
R-Square (COD)	0.99938
Adj. R-Square	0.99917

Equation	$y = a + b \cdot x$
Plot	UCPL intensity
Weight	No Weighting
Intercept	-9.13981 ± 0.241
Slope	2.03955 ± 0.1121
Residual Sum of Squares	0.00356
Pearson's r	0.9955
R-Square (COD)	0.99102
Adj. R-Square	0.98803

Figure S3. Statistical parameters for the fitting curves of the threshold excitation intensity (I_{th}) when excited with 532 nm light). (a) DPA 100 μM and (b) 9-PA 100 μM and PtOEP 1 μM in deaerated THF.

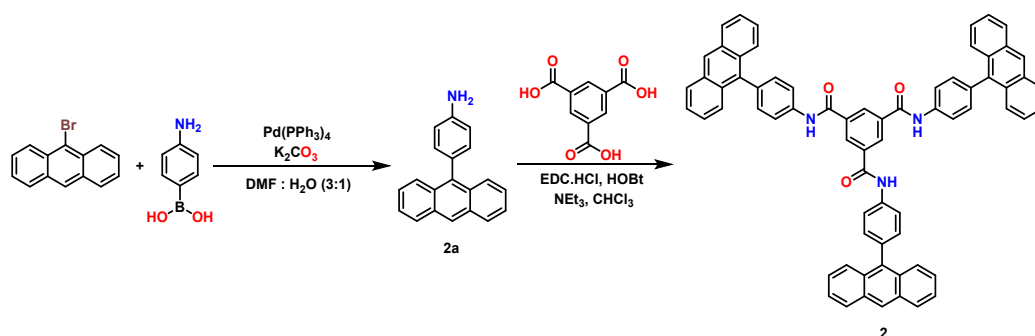
2. Synthesis of compounds 1, 2 and 3

Synthesis procedure for 1:



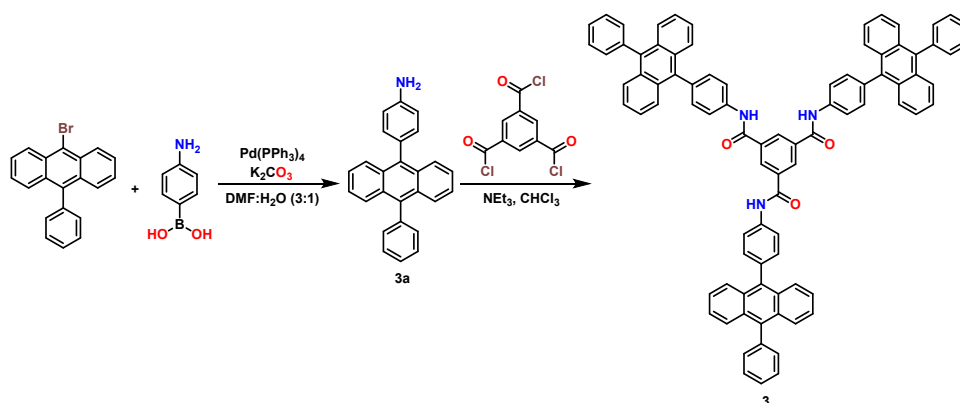
Synthetic Procedure: Compound **1a** was synthesized following the standard procedure reported elsewhere.^[1] In the next step, **1a** (600 mg, 2.01 mmol), EDC·HCl (582.7 mg, 3.04 mmol), HOBt (410.8 mg, 3.04 mmol) were taken in a 250 mL three-necked round-bottomed flask, and to it anhydrous CHCl_3 (50 mL) and NEt_3 (0.74 mL, 5.4 mmol) were added through septa. The reaction was kept for stirring at room temperature for 2.5 hours in argon atmosphere and then tris(2-aminoethyl)amine (0.11 mL, 0.60 mmol) was added and stirring was continued at room temperature for next 24 hours. The crude product was extracted using CHCl_3 and water and was further purified by column chromatography using silica gel (60-120 mesh) as stationary phase and $\text{CHCl}_3/\text{MeOH}$ mixture as the eluent. **Yield:** 58%, **R_f** = 0.35 (5% DCM/MeOH), **MP** = 217 °C, **¹H NMR** (DMSO-d_6 , 400 MHz): δ = 2.90 (t, 6H), 3.58 (t, 6H), 7.22 (t, 6H), 7.42(m, 19H), 8.12 (t, 12H), 8.65 (s, 5H). **¹³C NMR** (CDCl_3 , 100MHz): δ = 168.03, 142.36, 135.31, 132.91, 131.39, 131.13, 131.03, 129.59, 128.25, 128.13, 127.44, 126.81, 126.21, 126.03, 125.42, 125.36, 125.02, 124.92. **MS (m/z)** : Calculated for $\text{C}_{69}\text{H}_{54}\text{N}_4\text{O}_3$, 986.22[M] , found, 987.28 $[\text{M}+\text{H}]^+$, 1009.37 $[\text{M}+\text{Na}]^+$.

Synthesis procedure for 2:



Synthetic Procedure: Compound 2a was synthesized following the standard procedure reported elsewhere.^[2] In the next step, 1, 3, 5-benzenetricarboxylic acid (310 mg, 0.73 mmol), EDC. HCl (1.35 g, 4.5 mmol), HOBT (890 mg, 4.5 mmol) were taken in a 250 mL three-necked round-bottomed flask, and to it anhydrous CHCl_3 (50 mL) and NEt_3 (2 mL) were added using septa and the reaction was kept for stirring at room temperature for 4 hours in argon atmosphere. Compound 2a (1.20g, 2.42 mmol) was added to the above stirring solution and the reaction was refluxed for 48 hours. Extraction was done using CHCl_3 and H_2O in a separating funnel. CHCl_3 layer was collected, dried over Na_2SO_4 and evaporated using a rotary evaporator to get the crude product which was further purified by column chromatography (Silica, CHCl_3). Yield: 48% , $R_f = 0.75$ (CHCl_3). **MP** = 248 °C, $^1\text{H NMR}$ (DMSO-d_6 , 400 MHz): δ = 10.94 (s, 3H), 8.91 (s, 3H), 8.71 (s, 3H), 8.17 (m, 12H), 7.48-7.66 (m, 24H). $^{13}\text{C NMR}$, (DMSO-d_6 , 100 MHz): δ = 165.38, 139.02, 136.57, 133.90, 131.81, 131.42, 130.17, 128.92, 126.57, 126.33, 125.80, 120.98. **MS (m/z)** : calculated for $\text{C}_{69}\text{H}_{45}\text{N}_3\text{O}_3$, 963.27[M]; found; 963.27, $[\text{M}+\text{H}]^+$, 964.27.

Synthesis procedure for 3:



Synthetic Procedure: Compound 3a was synthesized following the procedure like compound 2a. Compound 3a (800 mg, 2.31mmol) was added to a round bottom flask containing dry CHCl_3 (50 ml). To this solution, NEt_3 (0.87 ml, 6.30 mmol) was added and the mixture was stirred at room temperature

for about 30 minutes and then cooled under ice bath. Reactant 1,3,5-benzenetricarbonyl trichloride (184.73 mg, 0.70 mmol) was then added and the reaction was kept for stirring for next 24 hours with gradual heating to room temperature. Crude product was extraction using CHCl_3 and purified by column chromatography using silica gel (60-120 mesh) as stationary phase and $\text{CHCl}_3/\text{MeOH}$ mixture as the eluent. **Yield:** 60 %, **R_f** = 0.80 (CHCl_3). **MP** = Above 300 °C. **¹H NMR** (DMSO-d_6 , 400 MHz): δ = 10.97 (s, 3H), 8.82-8.94 (m, 3H), 8.11-8.14 (s, 6H) , 7.47-7.71 (m, 45H). **¹³C NMR**, (CDCl_3 , 100 MHz): δ = 165.16, 138.81, 136.51, 135.97, 131.73, 131.12, 129.87, 129.74, 128.34, 126.85, 124.95, 120.50. **MS (m/z)** : calculated for $\text{C}_{87}\text{H}_{57}\text{N}_3\text{O}_3$, 1191.35[M]; found; 1191.40 [M]⁺, 1192.40 [M+H]⁺.

3. Concentration dependent UV-Vis. Absorption and emission spectra

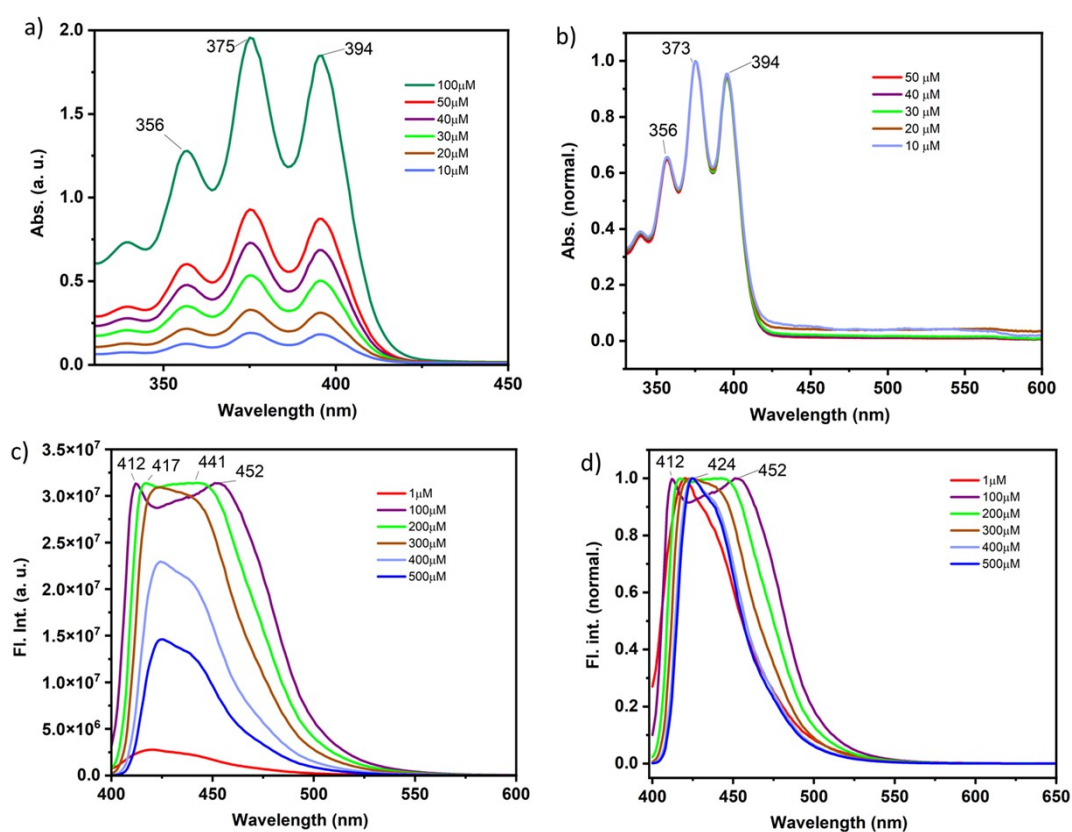


Figure S4: Plots (a) and (b) showing regular and normalized absorption spectra of molecule 3 in THF at concentrations of 10 μM , 20 μM , 30 μM , 40 μM , 50 μM , and 100 μM . Plots (c) and (d) showing regular and normalized emission spectra (λ_{ex} = 365 nm) of molecule 3 in THF at 1 μM , 100 μM , 200 μM , 300 μM , 400 μM , and 500 μM concentrations.

4. Concentration dependent ^1H NMR spectra

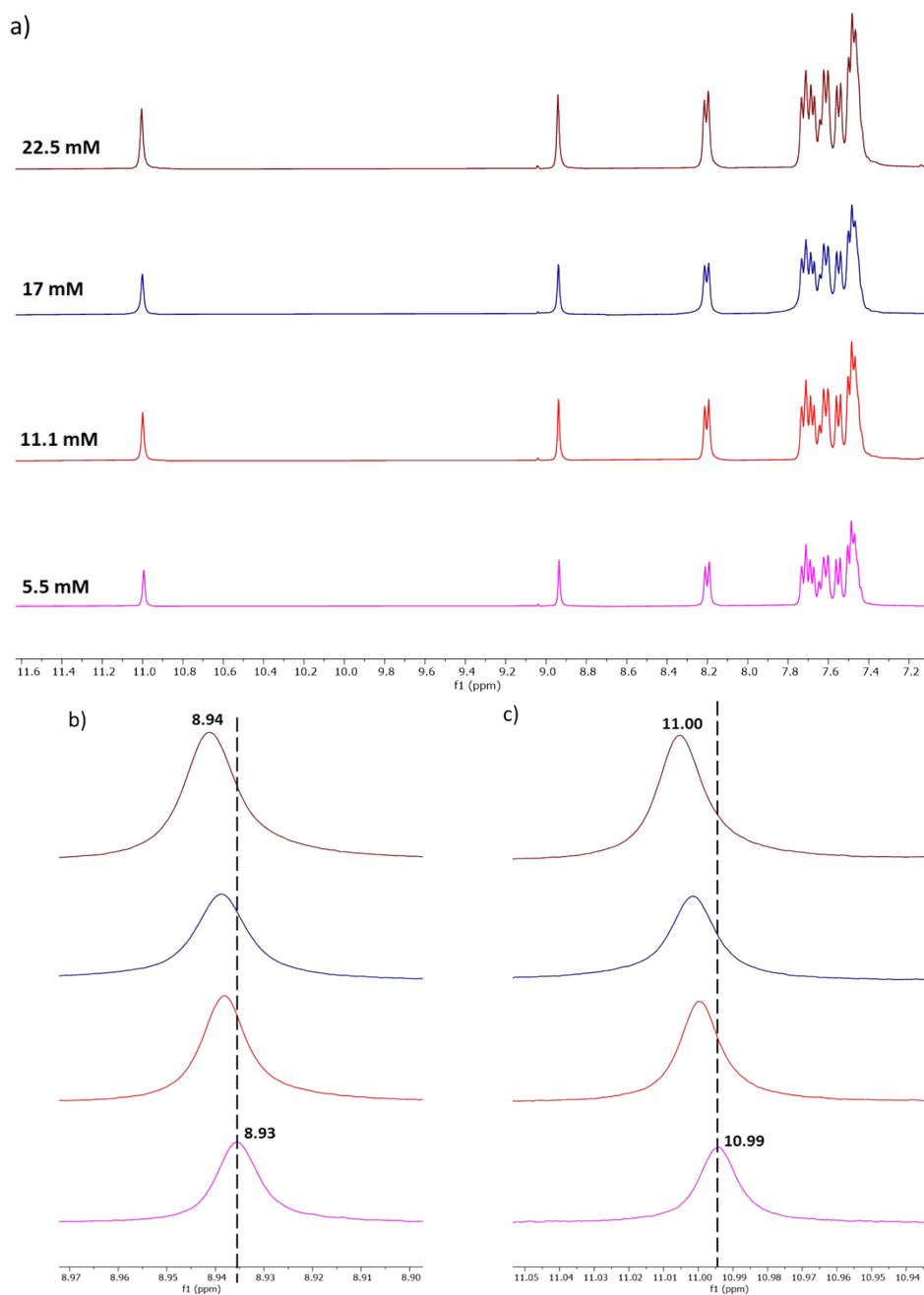


Figure S5: (a) Concentration dependent ^1H NMR (400 MHz) spectra of molecule **3** ($\text{DMSO-}d_6$, RT). Figures (b) and (c) showing the magnified parts for amidic and central benzene's proton positions.

5. Geometry optimized structures of molecules 1-3

Geometry was optimized by performing Density Functional Theory calculations (DFT) using Gaussian 09 software package.^[3] The most stable ground state geometries of all the molecules were obtained using B3LYP hybrid exchange-correlation functional in conjugation with 6-311G basis set in gas phase.

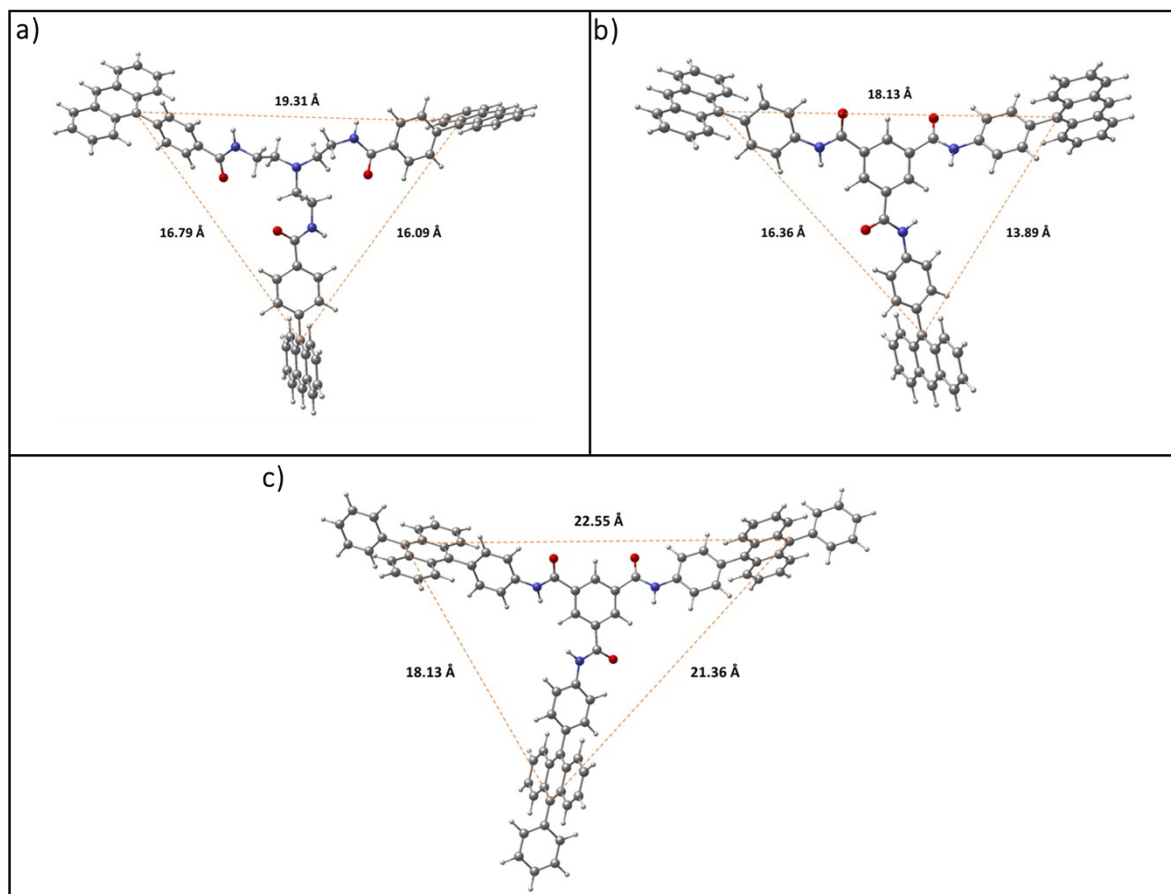


Figure S6: Images (a), (b) and (c) show geometry optimized structures of molecules 1, 2, and 3, respectively.

6. ^1H -NMR Spectra:

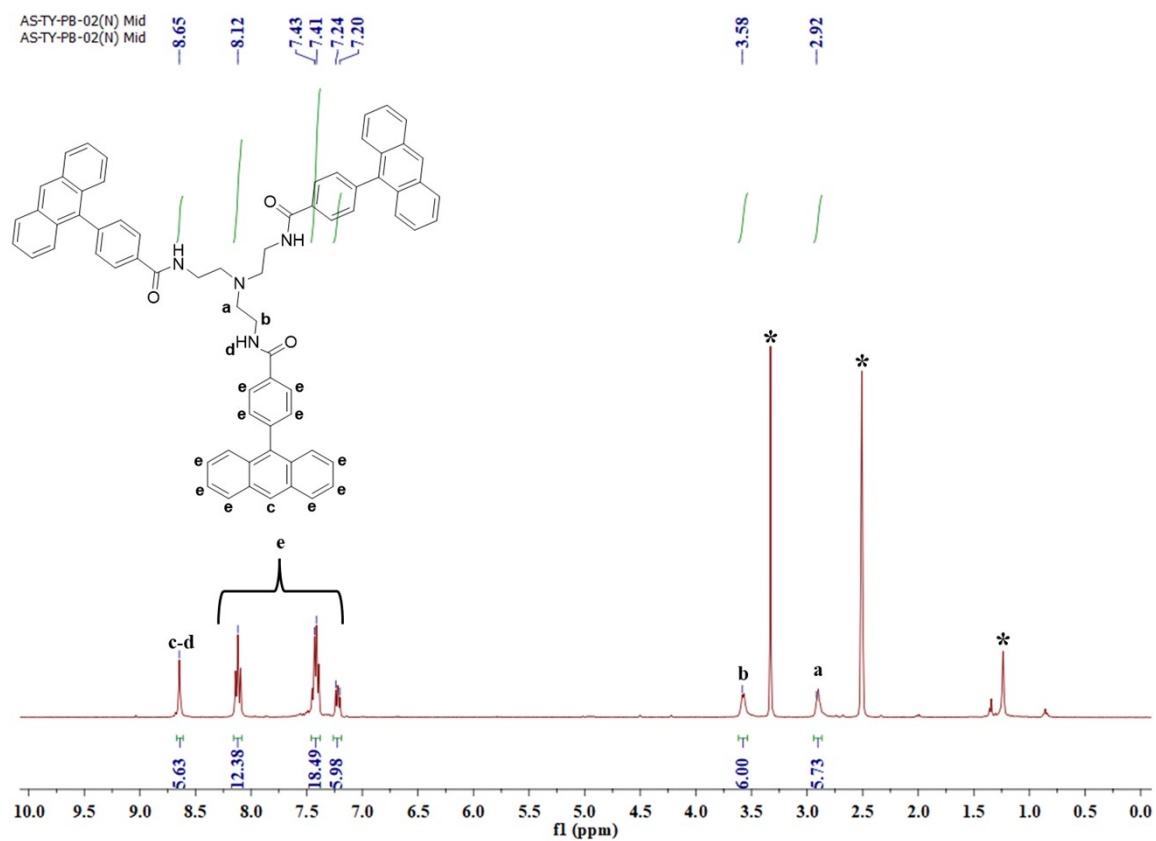


Figure S7: ^1H -NMR (400 MHz) Spectrum of compound **1** in $\text{DMSO}-d_6$ (* indicates peaks from residual solvent)

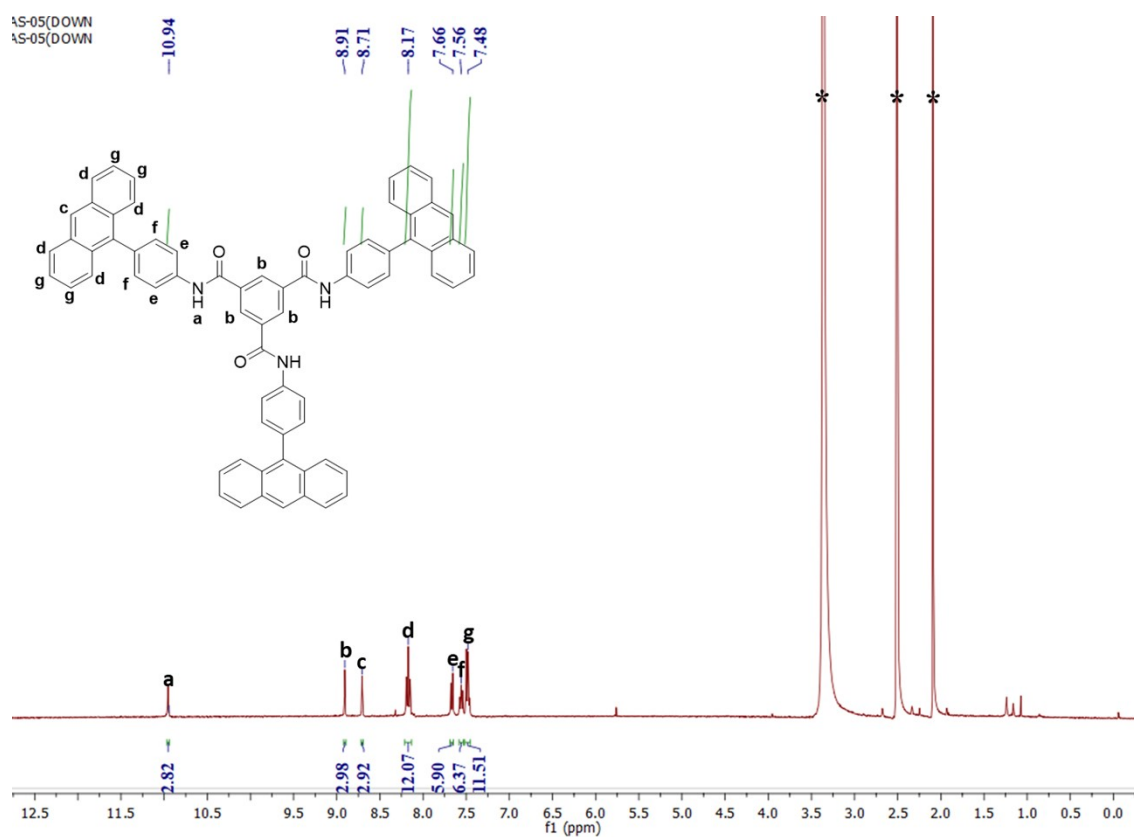


Figure S8: ¹H-NMR (400 MHz) Spectrum of compound 2 in DMSO-d₆ (* indicates peaks from residual solvent)

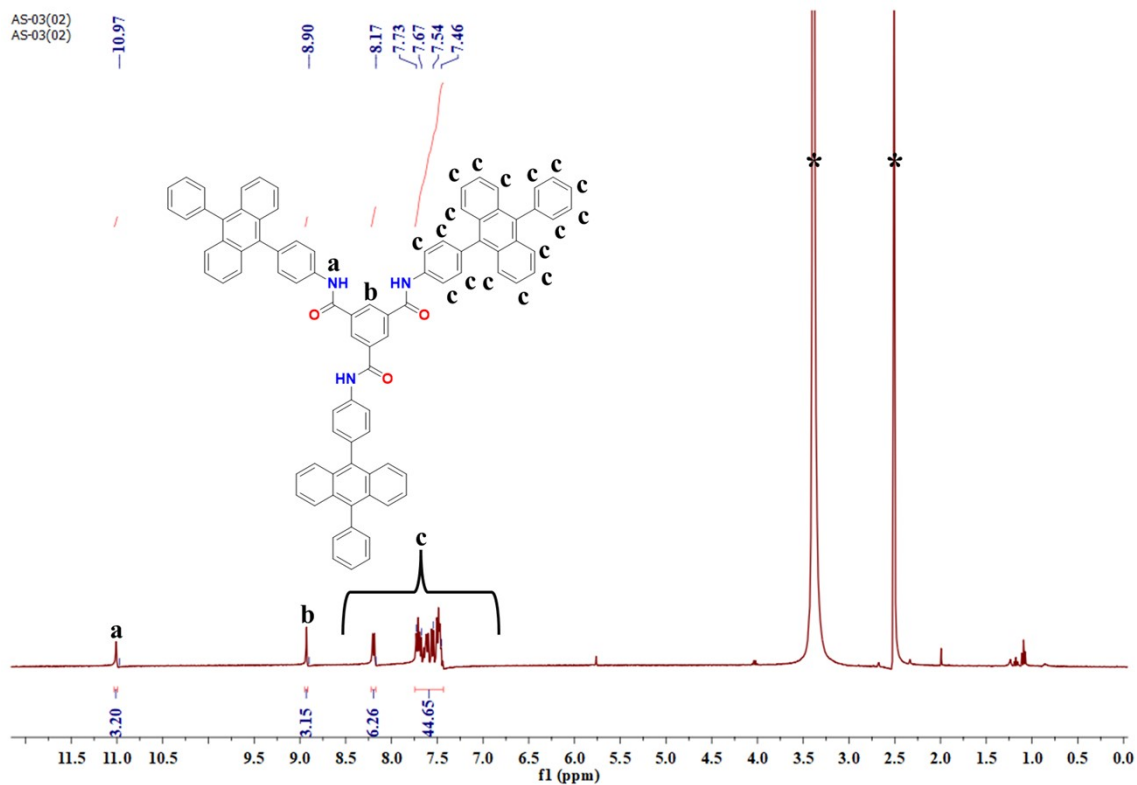


Figure S9: ¹H-NMR (400 MHz) Spectrum of compound 3 in DMSO-d₆ (* indicates peaks from residual solvent)

7. ^{13}C -NMR Spectra:

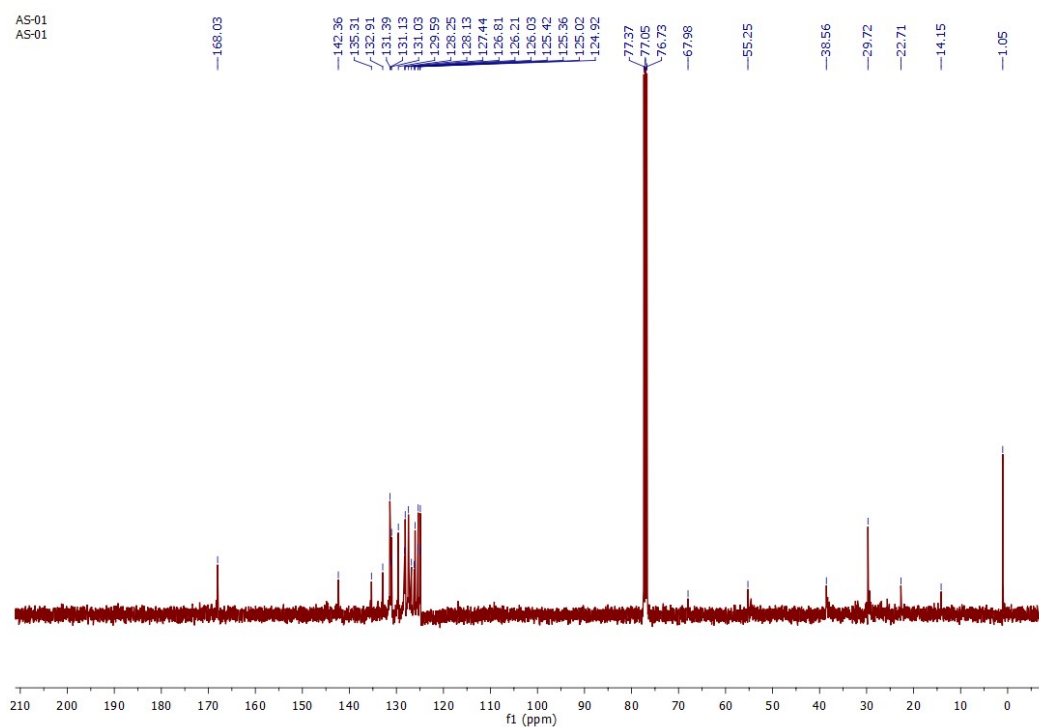


Figure S10: ^{13}C -NMR (100 MHz) Spectrum of compound **1** in CDCl_3 .

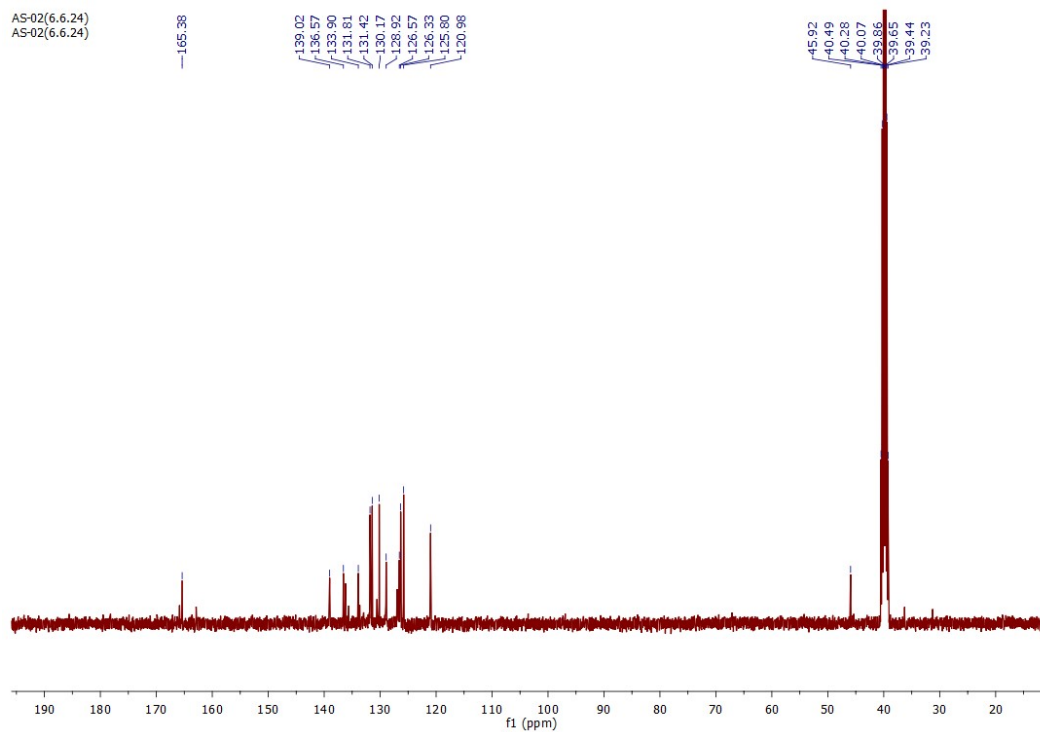


Figure S11: ^{13}C -NMR (100 MHz) Spectrum of compound **2** in $\text{DMSO}-d_6$.

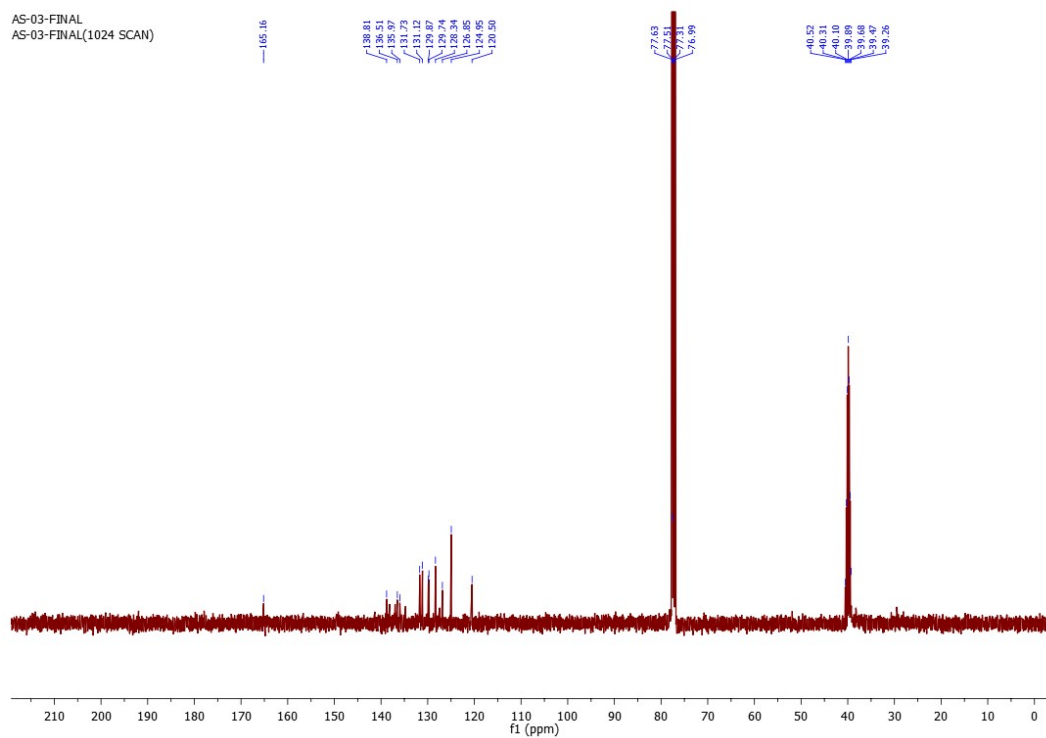


Figure S12: ^{13}C -NMR (100 MHz) Spectrum of compound **3** in CDCl_3 .

8. Mass Spectra of molecules 1-3

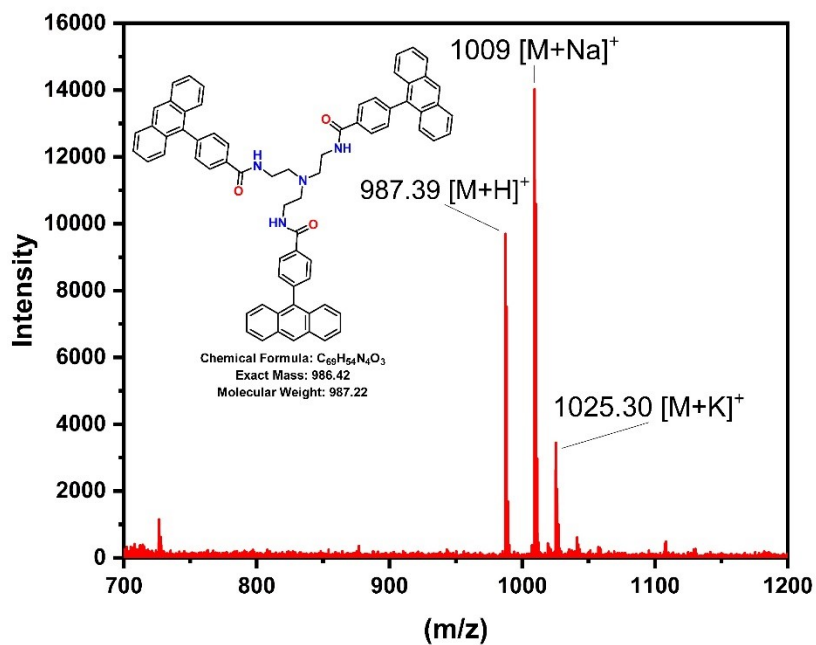


Figure S13: MALDI-MS Spectrum of compound **1**.

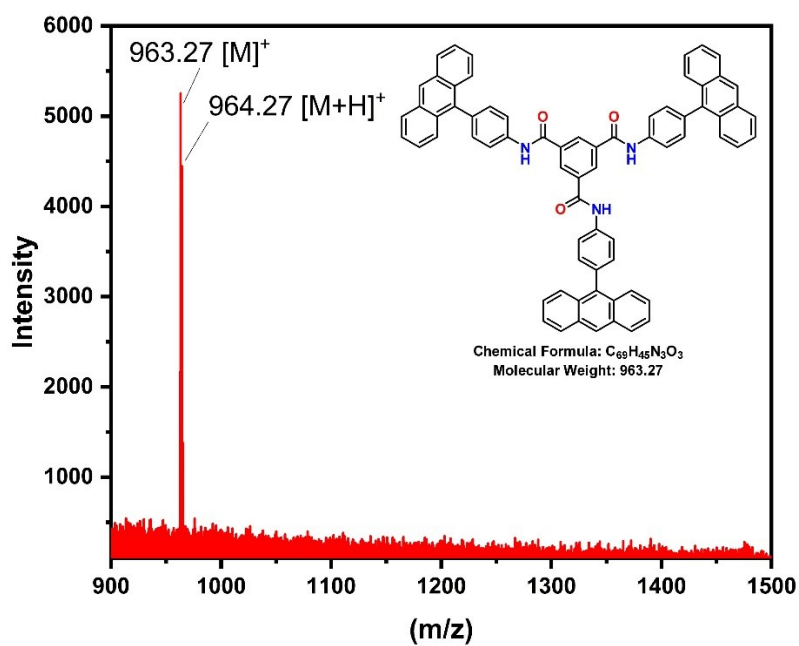


Figure S14: MALDI-MS Spectrum of compound 2.

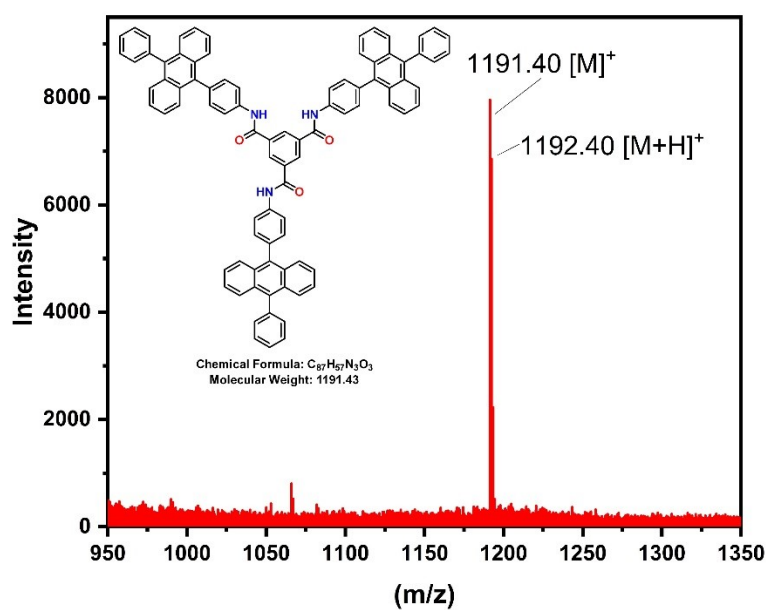


Figure S15: MALDI-MS Spectrum of compound 3.

9. References:

1. J. Hirokuni; K. Min-Tzu; D. Guerzo, André; Y. Yudai; M. Takuya; T. Makoto; I. Hirotaka, Tunable Stokes shift and circularly polarized luminescence by supramolecular gel, *J. Mater. Chem. C*, **2015**, 3, 5970–5975.
2. X. Liu, P. Dai, T. Gu, Q. Wu, H. Wei, S. Liu, K. Y. Zhang, Q. Zhao, Cyclometalated iridium(III) complexes containing an anthracene unit for sensing and imaging singlet oxygen in cellular mitochondria, *J. Inorg. Biochem.*, **2020**, 209, 111106.
3. Gaussian 09, M. J. Frisch, G. W. Trucks, H. B. Schlegel, G. E. Scuseria, M. A. Robb, J. R. Cheeseman, G. Scalmani, V. Barone, B. Mennucci, G. A. Petersson, H. Nakatsuji, M. Caricato, X. Li, H. P. Hratchian, A. F. Izmaylov, J. Bloino, G. Zheng, J. L. Sonnenberg, M. Hada, M. Ehara, K. Toyota, R. Fukuda, J. Hasegawa, M. Ishida, T. Nakajima, Y. Honda, O. Kitao, H. Nakai, T. Vreven, J. A. Montgomery, Jr., J. E. Peralta, F. Ogliaro, M. Bearpark, J. J. Heyd, E. Brothers, K. N. Kudin, V. N. Staroverov, R. Kobayashi, J. Normand, K. Raghavachari, A. Rendell, J. C. Burant, S. S. Iyengar, J. Tomasi, M. Cossi, N. Rega, J. M. Millam, M. Klene, J. E. Knox, J. B. Cross, V. Bakken, C. Adamo, J. Jaramillo, R. Gomperts, R. E. Stratmann, O. Yazyev, A. J. Austin, R. Cammi, C. Pomelli, J. W. Ochterski, R. L. Martin, K. Morokuma, V. G. Zakrzewski, G. A. Voth, P. Salvador, J. J. Dannenberg, S. Dapprich, A. D. Daniels, O. Farkas, J. B. Foresman, J. V. Ortiz, J. Cioslowski, and D. J. Fox, Gaussian, Inc., Wallingford CT, 2009.
4. T. N. Singh-Rachford, F. N. Castellano, Photon upconversion based on sensitized triplet–triplet annihilation. *Coord. Chem. Rev.* **2010**, 254, 2560-2573.
5. N. Yanai, K. Suzuki, T. Ogawa, Y. Sasaki, N. Harada, N. Kimizuka, Absolute Method to Certify Quantum Yields of Photon Upconversion via Triplet-Triplet Annihilation. *J. Phys. Chem. A* **2019**, 123, 10197-10203.
6. A. Olesund, V. Gray, J. Mårtensson, B. Albinsson, Diphenylanthracene Dimers for Triplet–Triplet Annihilation Photon Upconversion: Mechanistic Insights for Intramolecular Pathways and the Importance of Molecular Geometry. *J. Am. Chem. Soc.* **2021**, 15, 5745–5754.